

23

N91-30239

RAPID THERMAL CYCLING OF SOLAR ARRAY BLANKET COUPONS
FOR SPACE STATION FREEDOM

David A. Scheiman *
Sverdrup Technology, Inc.
Brook Park, Ohio

Bryan K. Smith
NASA Lewis Research Center
Cleveland, Ohio

ABSTRACT

NASA Lewis Research Center has been conducting rapid thermal cycling on blanket coupons for Space Station Freedom. This testing includes two designs (8 coupons total) of the solar array. Four coupons were fabricated as part of the Photovoltaic Array Environmental Protection Program (PAEP), NAS3-25079, at Lockheed Missiles and Space Company. These coupons began cycling in early 1989 and have completed 172,000 thermal cycles. Four other coupons were fabricated a year later and included several design changes; cycling of these began in early 1990 and has reached 90,000 cycles. The objective of this testing is to demonstrate the durability or operational lifetime (15 yrs.) of the welded interconnects within a Low Earth Orbit (LEO) thermal cycling environment. The paper presented describes the blanket coupons, design changes, test description, status to date including performance and observed anomalies, and any insights related to the testing of these coupons. The paper also includes the description of a third design.

INTRODUCTION

Power for Space Station Freedom (SSF) will be generated by four photovoltaic power modules which each employ two solar array wings. The solar array wings are comprised of two blankets that each are an assembly of 82 active solar panels. A panel contains 200 solar cells in series, with each cell connected to an underlying circuit interconnect by 10 welded contact points. The peak power output for each cell is slightly over 1 watt. The on-orbit deployed envelope of the solar array wing is 38 ft. by 110 ft.

SSF will have an operating altitude range of 180 to 240 nautical miles at an inclination of 28.5 degrees. At this altitude SSF will orbit the earth approximately once every 90 minutes or 6000 times per year. With each orbit SSF will pass into and out of the sun's view causing temperature excursions of over 160°C. These temperature extremes can induce thermal stresses in the blanket materials of the array and can, over time, result in structural fatigue of the panel components. This is just one of the many detriments of the low earth orbit (LEO) space environment which include atomic oxygen, micrometeoroids, vacuum, plasma, and radiation.

The thermal stresses induced on the array blanket are the focus of rapid thermal cycling. Different materials of the array have different coefficients of thermal

* Work supported under NASA Lewis contract NAS3-25266

expansion (CTE); for example, silicon is 2×10^{-6} (cm./cm.)/°C and Kapton (ref 1) is 26×10^{-6} (cm./cm.)/°C. Various CTE's for different materials used in the array blanket can be seen in Figure 1 (ref. 2). The resultant effects of thermal stresses are difficult to predict and therefore warrant physical testing. In addition to verifying mechanical integrity, thermal cycling data will also serve to verify assumptions used in calculating array performance over the design lifetime.

Solar array blanket coupons have been tested to 172,000 cycles for 1989 samples and 90,000 cycles for 1990 samples. Both of these sample groups have had only slight degradation in performance. A third test coupon which represents the latest design has completed 6,000 cycles. These coupons will also run to 90,000 cycles.

TEST ARTICLE DESCRIPTION AND DESIGN EVOLUTION

All of the coupons used for testing were fabricated by Lockheed Missiles and Space Company (LMSC) under the Photovoltaic Array Environmental Protection Program (PAEP), NAS3-25079. Between 1989 and 1991 three different designs, designated blanket design I (SSF 1989), II (SSF 1990) and III (SSF 1991), were delivered to NASA-LeRC for thermal cycle testing. Four coupons of each design were delivered, the cells used for these coupons are secondary cells and therefore efficiency is below nominal.

Each coupon contains four 8x8 cm silicon solar cells with CMX coverglass connected in series. The coverglass is bonded to the solar cell with Dow Corning DC93-500 silicone adhesive. The SSF solar cells are an N on P type silicon cell with a boron back surface field (BSF) and a 10 ohm-cm nominal base resistivity. The collection grids and contact points are layers of titanium, palladium, aluminum and silver. Four holes in the cell bring the front N contacts through to the back side where they are welded to the copper circuitry along with the six P backside contacts. Solar cells for SSF will be supplied by both Applied Solar Energy Corporation and Spectrolab Inc.

It is difficult to assess the integrity of a solar cell weld without destructive testing. One solar array wing alone will contain over 164,000 cell to circuit welds, therefore, LMSC must maintain tight control over their production welding operation to assure adequate welding. LMSC addressed this in the PAEP program by completing a weld optimization task. The task determined voltage, emissivity, and IR sensing settings that will be used to control the weld pulse energy and duration on the production welders. Pull tests, photomicrographs, thermal cycling and illumination tests were used to evaluate the quality of the solar cell to copper interconnect weld. From this effort a weld schedule was selected that exhibited statistically the highest pull strengths and showed no obvious failure mechanisms such as gross melting, voids,

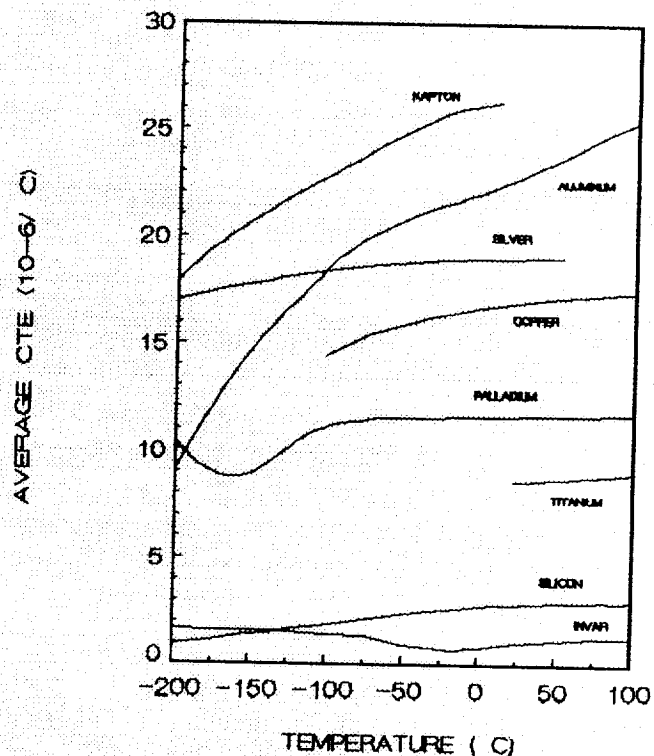


Figure 1: CTE vs. Temperature for Solar Array Materials

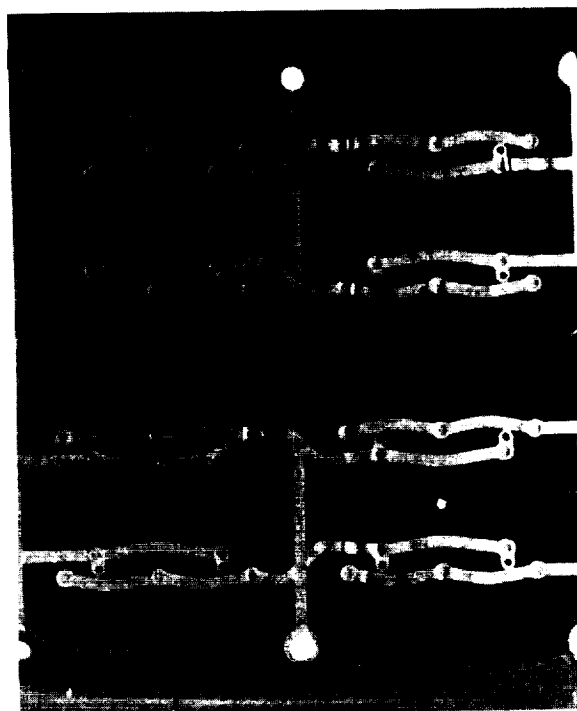
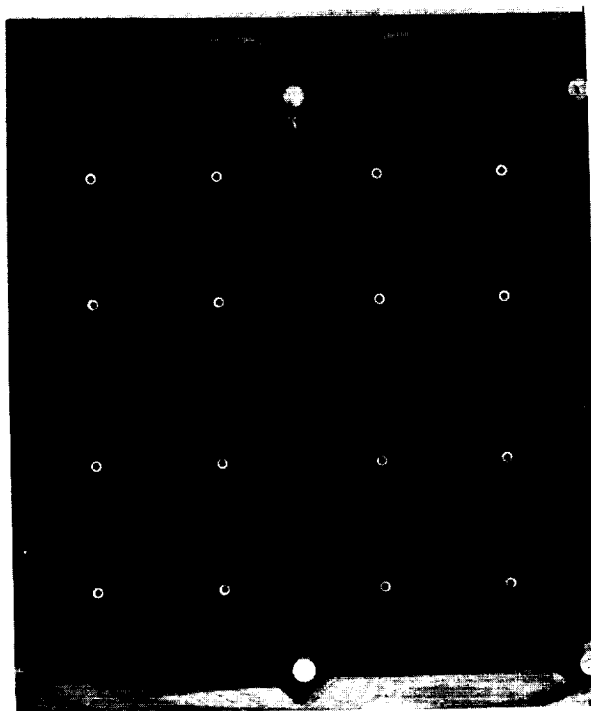


Figure 2: SSF 1989 (design I) Test Coupon -- Front and Back

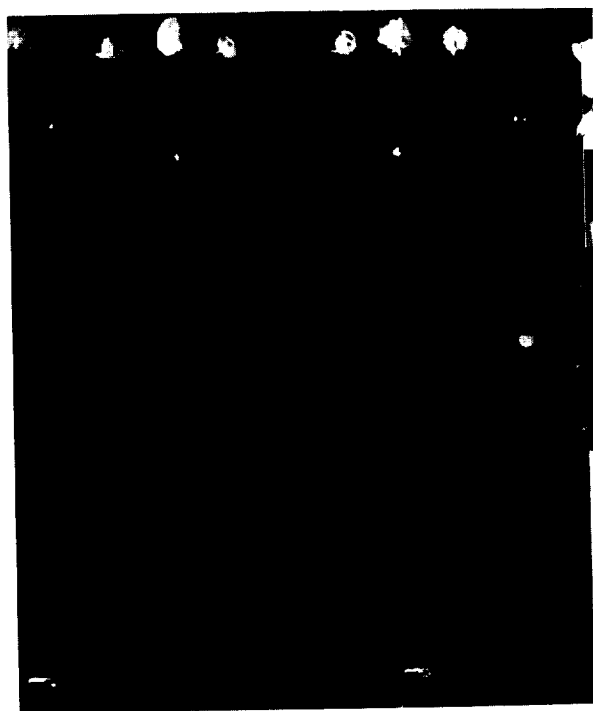
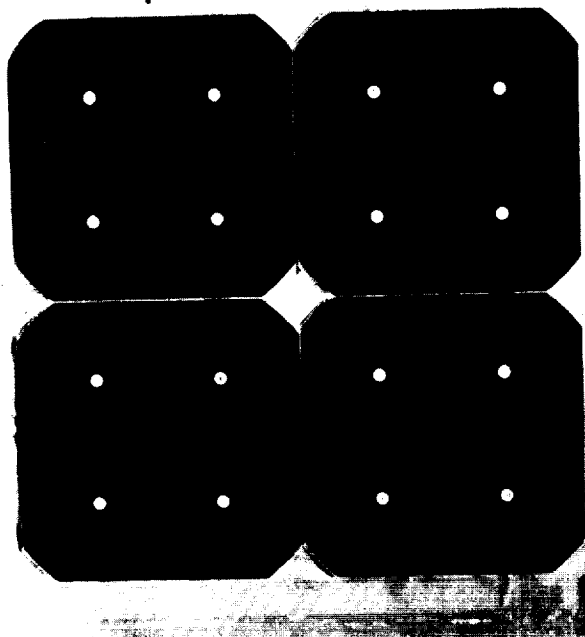


Figure 3: SSF 1990 (design II) Test Coupon -- Front and Back

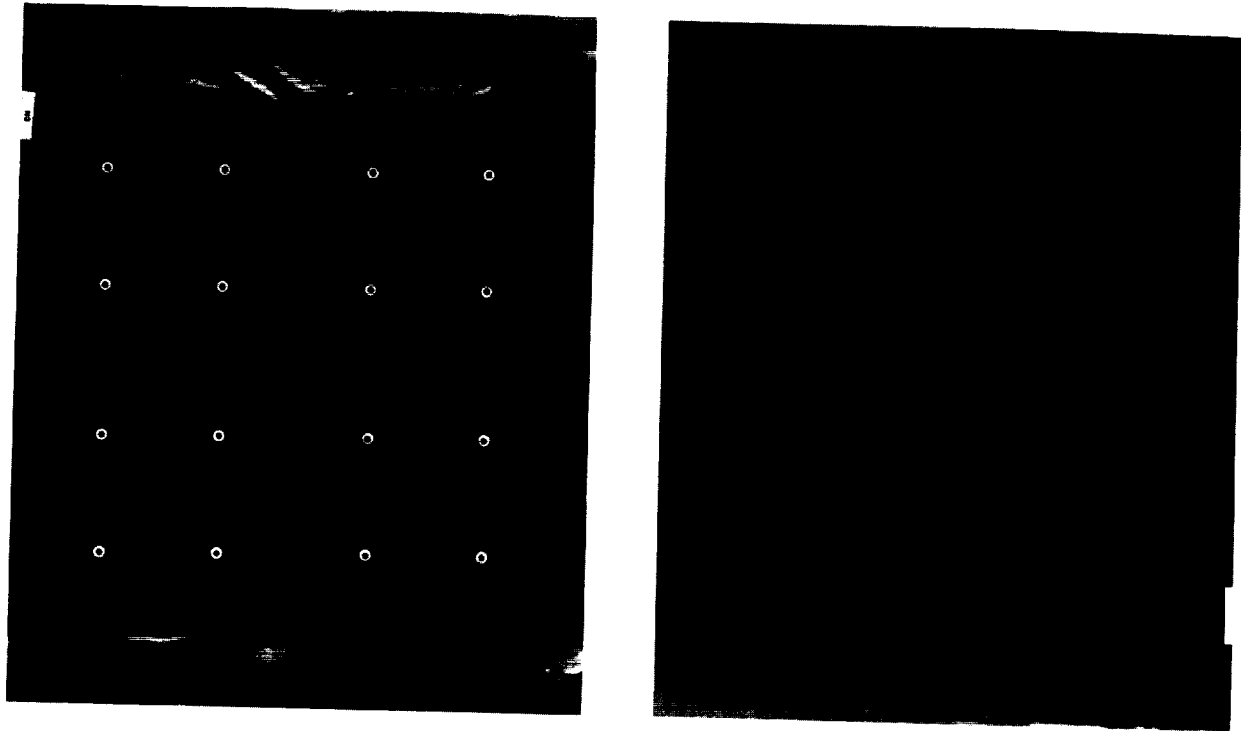


Figure 4: SSF 1991 (design III) Test Coupon -- Front and Back

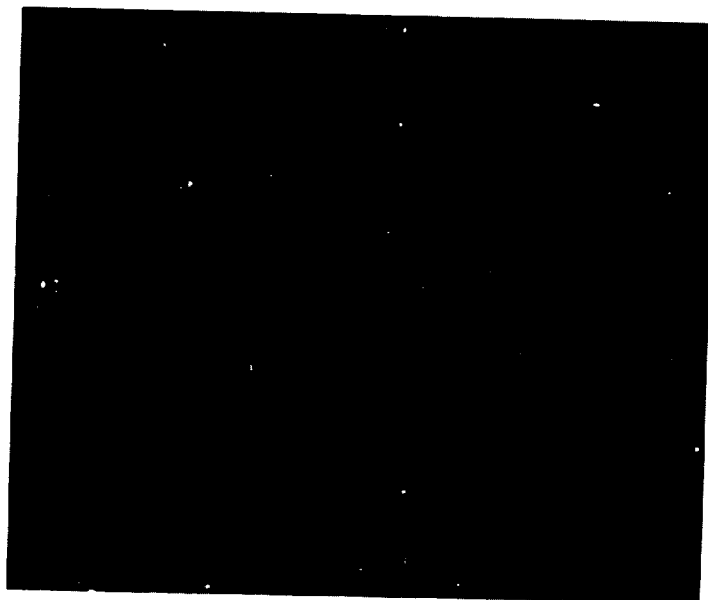


Figure 6: Copper Fatigue of SSF 1989 at 150,000 cycles

or cracking. In addition to deriving a weld schedule and closely monitoring the weld parameters, thermal cycling will also be used throughout the production process to assure quality welds.

Blanket design I employed two layers of Kapton H polyimide film with the copper circuit in between the layers (Fig. 2). The first layer of Kapton was cut to insulate the cell from the copper circuitry and allow the second layer of Kapton an adhesive bond path to the back of the solar cell. The copper circuitry was bonded to the first layer of Kapton with a polyester adhesive. The solar cells were welded to the circuitry through access holes in the first layer of Kapton. The second layer of Kapton or coverlay provides the structural component for the blanket and also contains the Kapton hinge loops that are used to connect the panels together to form the blanket assembly. The second sheet of Kapton is bonded with DC93-500 to the exposed circuitry, the first layer of Kapton and the back of the solar cells.

Atomic oxygen protection on blanket design I was achieved by coating both layers of Kapton on both sides with 1300 angstroms of silicon dioxide. The coupons were also configured with aluminum foil covered Kapton hinges. The aluminum foil was considered the most effective way of protecting the critical hinge area from atomic oxygen.

Blanket design II coupons substituted the Kapton H with an experimental atomic oxygen resistant Kapton (AOR Kapton) (Fig. 3). The solar cells were changed to include redundant weld contact points that allowed for repair or replacement of a solar cell once it had been welded into a panel assembly. The copper circuitry was also changed to control adhesive flow in the manufacturing process and to accommodate the redundant weld contact. Two of the four design II coupons delivered featured bypass diodes that are used within the flexible panel assemblies to protect individual solar cells from reverse biasing resulting from transitory shadowing. The SSF design will use one bypass diode every eighth solar cell which will also provide a shunt path if an open circuit develops within an eight cell unit. The diodes used on design II had Kovar leads and were welded to the circuitry in four places.

Blanket design III coupons returned to the silicon dioxide coated Kapton H for the copper circuit layer but replaced the back surface Kapton with a laminate (Fig. 4). The laminate consists of two layers of silicon dioxide coated Kapton with a glass scrim cloth bonded in between the layers. Development tests have demonstrated that this design will provide adequate atomic oxygen protection to the blanket over the 15 year design lifetime. The coupons also incorporated additional copper circuitry under the bypass diode that will act as a sink and allow the diode to operate at a reduced temperature. Two of the four design III coupons have bypass diodes with copper leads.

TEST DESCRIPTION

TEST CHAMBER

The thermal cycling chamber, Figure 5, is designed to cycle a test article between two temperature extremes. The chamber consists of two smaller chambers that each maintain a constant hot and cold temperature. Test frames are installed in the chamber and are the vehicle by which the test articles are moved between the hot and cold chambers. The movement of the frames is controlled by a computer which receives temperature information from a thermocouple mounted on each test article. When a given temperature is achieved, the computer activates the movement of the test frame to the adjacent chamber. Test frames are individually controlled and switching depends only on temperature. One thermal cycle is the completion of exposure to both temperature extremes. Cycle times range from 2 to 5 minutes and can vary depending on coupon mass and chamber temperature. Because the chamber is computer controlled, timed cycling and limited temperature profiling can also be used.

The thermal cycling test rig is an insulated box with an oven over a freezer. The oven is heated using two 500 watt resistive heaters which provide radiative and

convective heat. The freezer is cooled using liquid nitrogen fed directly into the chamber. This also supplies an inert atmosphere for both chambers. The system is capable of temperature extremes between $+120^{\circ}\text{C}$ and -180°C with a 10° gradient in either chamber. Disadvantages of this method include the lack of information regarding the effects of outgassing of the components, stresses due to pressure differentials, and local temperature gradients (ref. 3).

Up to four 8" x 8" x .5" solar array test articles can be tested simultaneously. Temperatures are read at approximately 16 second intervals and cycle counts are printed hourly. The chamber shuts down automatically when cycling is completed. At set intervals, the test articles are removed from the chamber for performance testing and visual inspection.

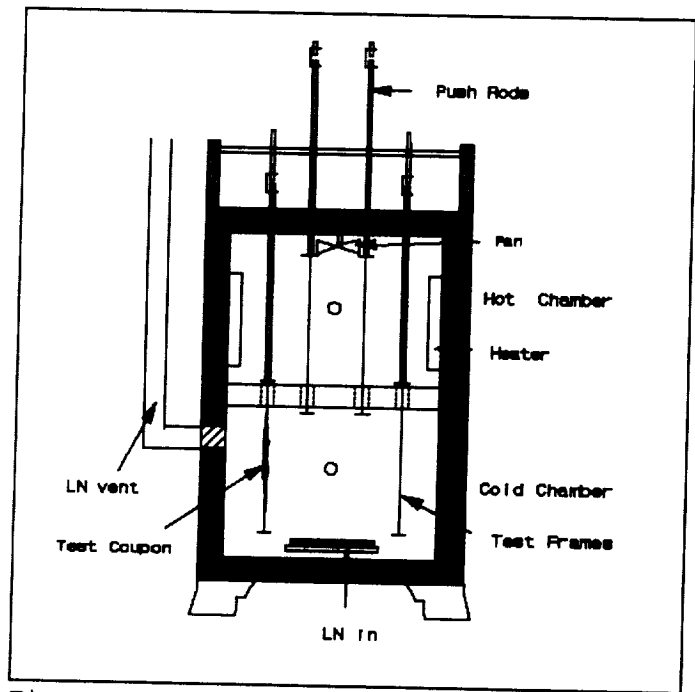


Figure 5: Thermal Cycling Chamber cross-section

ARRAY PERFORMANCE

Performance of the test article is measured by the range of its electrical power output under illumination. This power output is characterized as a curve of current vs. voltage or an I-V curve. The I-V curve is generated by varying a load constant of 1.36 mW/cm^2 is used in efficiency calculations. The array efficiency is also based on the cell area only. The following information from the I-V curve is used in performance evaluation: short circuit current in amps, denoted I_{sc} ; open circuit voltage in volts, denoted V_{oc} ; current at maximum power out in amps, denoted I_{max} ; voltage at maximum power out in volts, denoted V_{max} ; maximum power out in watts, denoted P_{max} ; fill factor, denoted FF; peak efficiency in percent, denoted eff.; measured peak power over initial peak power, denoted P/P_0 .

I-V curves were obtained by flash testing. Flash testing is performed by using a short burst of light (Xenon arc lamp) with a normalized solar intensity at air mass zero (AM0). A complete I-V curve containing 30-80 data points is generated in about 1.5 milliseconds. This flash test provides curve data with virtually no heat generated in the array and therefore data comparisons can be made because repeatability is very good. This measurement is performed at room temperature with the coupons removed from the chamber.

If an interconnect failure were to occur in the array, series resistance would increase. Series resistance would most prominently affect the slope of the I-V curve between P_{max} and V_{oc} and would result in a drop in FF and P_{max} . The coupons have electrical test pads after each cell in the series circuit that can be used to isolate failures to a single solar cell if a loss in performance is detected at the coupon level.

An additional check is made on samples which contain bypass diodes. The bypass diode is forward biased (array is reverse biased) and a dark I-V curve is created using a curve tracer with the coupons at room temperature. Any loss of continuity could easily be detected using this method.

SOLAR CELL VISUAL INSPECTION

In addition to performance characteristics, the solar array test coupons are visually inspected. The test coupons are viewed under 10X magnification with incident light at varying angles. Because of the coverglass and the reflective nature of the cell, light angles are varied to detect any flaws in the surface of the cell or coverglass. These flaws are mapped on a paper image of the cell and subscripted with the type of flaw and time observed. Both the front and back side of the test coupon are mapped. The following flaws are noted:

- 1) B -- break/crack in cell surface
- 2) C -- break/crack in coverglass
- 3) V -- void, open area i.e. lack of adhesive
- 4) W -- wrinkle in interconnect/ blanket
- 5) A -- adhesive, typical evidence of migration or elongation
- 6) O -- other, any other nonconformity in the cell; bubbles, contamination, peeling, delamination, etc.

Visual mapping with subscripted notations are performed at regularly scheduled intervals. Ultimately, the visual inspection is used to observe any trends that would lead to or cause performance degradation.

TEST RESULTS

Rapid thermal cycling of the solar array coupons for SSF has been an ongoing project for more than two years. Test articles have accumulated well over 500,000 cycles. Four 1989 coupons have been cycled to 90,000 cycles with two completing 172,000 cycles, two 1990 coupons have been cycled to 90,000 cycles, and four 1991 coupons are currently being tested. Based on this testing several observations have been made to establish confidence in the welded interconnects and array design.

Performance degradation was observed in both the 1989 and 1990 test coupons. The amount and rate of degradation varied between the two designs. Performance of the 1989 dropped less than 1% after 90,000 cycles (ref. 4) and was down 3% after 172,000 cycles. Performance of the 1990 coupons was down 2% after 66,000 cycles and 6% after 90,000 cycles. The 1991 coupons have just completed 6,000 cycles with no performance degradation. Overall performance parameters are included in Table 1.

Visual inspection of all the coupons revealed only very slight changes in the cells. Fine cracks were observed in the cell and coverglass. Most of the cracks were observed prior to cycling and only tended to elongate fractionally during the first 12,000 cycles. These changes in the cell were viewed as posing no threat to the integrity of the array.

The backside of the coupon, interconnect side, exhibited a change in the copper interconnects, Kapton, and adhesive layers. Within the first 12,000 cycles, motion of the copper and Kapton was evident. The copper went from being flat to having wrinkles or ripples. This out of plane rippling, resulting from initial thermal stresses, has actually provided a stress relief for subsequent thermal cycling. Rippling of the copper interconnects was random and even ran up to the weld joints. The adhesive also appeared to have elongated in some places. This elongation is characterized by round voids in the adhesive that have changed to oval shapes. The Kapton also wrinkled, which usually fit the mold of the underlying Kapton. After 12,000 cycles the motion continued but was stabilized, i.e. no significant changes in size or quantity were apparent. The 1990 coupon design had less adhesive area. This resulted in the Kapton pulling away from the cell in the four corners although the adhesive did retain the bond.

As the cycling and rippling continued, fatigue in the copper near the welds was more apparent. The copper areas around the weld were brittle due to the heating incurred during the weld process. In areas where the rippling was occurring at or close to the weld, copper fatigue resulted around the weld joint (Fig. 6). This was first observed after 150,000 cycles in the 1989 coupons and after 72,000 cycles in the

Table 1: Selected Solar Array Coupon Electrical Performance

SSF 1989 Test Coupons, Design I (SSFSA-4)

CYCLES :	0	30000	60000	90000	172000
Isc (A)	2.7070	2.6654	2.6759	2.6323	2.6504
Voc (V)	2.4470	2.5127	2.5097	2.4885	2.4454
Imax (A)	2.4740	2.3993	2.4368	2.3591	2.3329
Vmax (V)	1.8360	1.9289	1.9115	1.9028	1.9016
Pmax (W)	4.5430	4.6279	4.6580	4.4889	4.4363
F.F.	0.686	0.691	0.694	0.685	0.684
effic.	13.4 %	13.6 %	13.7 %	13.2 %	13.1 %
P/Po	1.0000	1.0187	1.0253	0.9881	0.9765

SSF 1990 Test Coupons, Design II (SSFSA-9)

CYCLES :	0	32000	66000	90000
Isc (A)	2.6158	2.6722	2.6211	2.6223
Voc (V)	2.4916	2.5013	2.5001	2.4615
Imax (A)	2.3397	2.3430	2.3058	2.3420
Vmax (V)	1.9078	1.9152	1.8979	1.7863
Pmax (W)	4.4636	4.4874	4.3761	4.1835
F.F.	0.685	0.671	0.668	0.648
effic.	13.2 %	13.2 %	12.9 %	12.3 %
P/Po	1.0000	1.0053	0.9804	0.9372

SSF 1991 Test Coupons, Design III (SSFSA-12)

CYCLES :	0	3000	6000 *
Isc (A)	2.6048	2.6722	2.4477
Voc (V)	2.4116	2.5013	2.1440
Imax (A)	2.2221	2.3430	2.0943
Vmax (V)	1.8173	1.9152	1.5460
Pmax (W)	4.0382	4.4874	3.24
F.F.	0.643	0.671	0.617
effic.	11.9 %	12.1 %	9.5 %
P/Po	1.0000	1.0162	-----

* data not accurate (non-uniform light source)

1990 coupons. The copper fatigue occurred primarily by the corner welds (P contacts) and was a result of less adhesive around that weld. The 1989 coupons had approximately 3 visible copper fatigue weld areas after 172,000 cycles and the 1990 coupons had approximately 16 copper fatigue weld areas. The 1990 coupons had considerably more copper fatigue failures due to the lack of stability in the AOR Kapton and the smaller adhesive area. The 1991 coupons utilize the Kapton H of the 1989 samples, however they will have the smaller adhesive area of the 1990 samples.

One of the 1990 coupons was assembled with a bypass diode. The diode was welded to the copper interconnect in four places, two on each side. After 72,000 cycles the weld connections completely separated although there was no loss of continuity. The cause for this separation was the thermal expansion mismatch between the copper interconnect and the Kovar lead of the diode. The 1991 coupons now use a bypass diode with a copper lead to match the interconnect.

CONCLUSIONS

Based upon test data from blanket design I and II coupons the SSF solar array will experience some performance degradation due to thermal cycling over the 15 year LEO mission. Performance degradation in the coupons can be attributed to a combination of fatigue cracks in the dimpled area of the copper interconnect adjacent to the solar cell weld and increased series resistance of the solar cells and interconnects.

Although the results represent a small statistical sample of the total welds on the SSF solar array, the test data strongly suggests that the weld between the solar cell and copper interconnect is adequate for the 15 year design life in LEO. However, repeatability in the welding process and sufficient adhesive distribution around the welds will be important to assure this in the production program. A transient plasticity analysis of the solar array blanket also indicated that the fatigue life of the solar array blanket should be higher than the program requirement (ref. 5). Considering blanket design I and II coupon test data, assembly level circuits and connections and a statistical treatment of the welding and manufacturing process, performance losses for the SSF solar array due to thermal cycling will be between 0.5% to 1% for 5 - 10 years and 1% - 2% for 10 to 15 years in LEO. Data for blanket design III will be available in December of 1991 and the final flight design is scheduled to begin thermal cycling testing at NASA-LeRc in April 1992.

REFERENCES

1. Kapton is a registered trademark of E. I. DuPont De Nemours and Co., Inc.
2. Jet Propulsion Laboratory: Solar Cell Array Design Handbook Volume II. NASA October 1976 pp. 7.11-4,5.
3. Brinkmann, P. W.; Reimann, J.: Efficient Thermal Cycling of Solar Panels in Solar Simulation Facilities With a Multi-Panel Test Rig. Proc. 2nd European Symposium "Photovoltaic Generators in Space", Heidelberg, 15-17 April 1980 (ESA SP-147, June 1980) pp. 195-197.
4. Scheiman, D. A.; Smith, B. K.; Kurland, R. M.; Mesch, H. G.: Rapid Thermal Cycling of New Technology Solar Array Blanket Coupons. 25th IECEC, Volume 1 pp. 575-580.
5. Armand, S. C.; Liao, M-H; Morris R. W.: A Transient Plasticity Study and Low Cycle Fatigue Analysis of Space Station Freedom Photovoltaic Solar Array Blanket. NASA LeRc Technical Memorandum 102516.

